

Electronic Supplementary Information (ESI)

Bipyridine bisphosphonate-based fluorescent optical sensor and optode for selective detection of Zn²⁺ ions and its applications

R. Selva Kumar^a, S.K. Ashok Kumar^{a*}, Kari Vijayakrishna^a, Akella Sivaramakrishna^a, Priyankar Paira^a
C.V.S. Brahmamanda Rao^b, N. Sivaraman^b, and Suban K. Sahoo^c

^a Department of Chemistry, School of Advanced Sciences, Vellore Institute of Technology, Vellore-632014, Tamil Nadu, India. E-mail: ashok312002@gmail.com.

^b Indira Gandhi Centre for Atomic Research, HBNI, Kalpakkam-603102, Tamil Nadu, India

^c Department of Applied Chemistry, S. V. National Institute Technology, Surat-395007, Gujarat, India

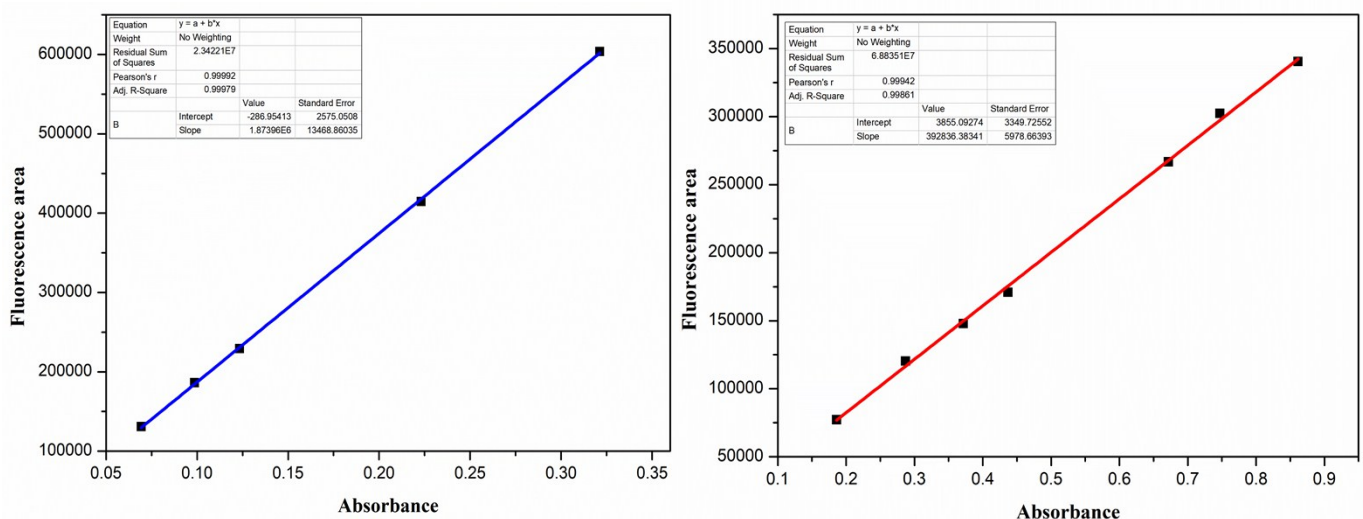


Figure 1S: Absorbance *verses* fluorescence of (a) 2-Amino pyridine in 1N H₂SO₄ (b) L-Zn²⁺ in acetonitrile.

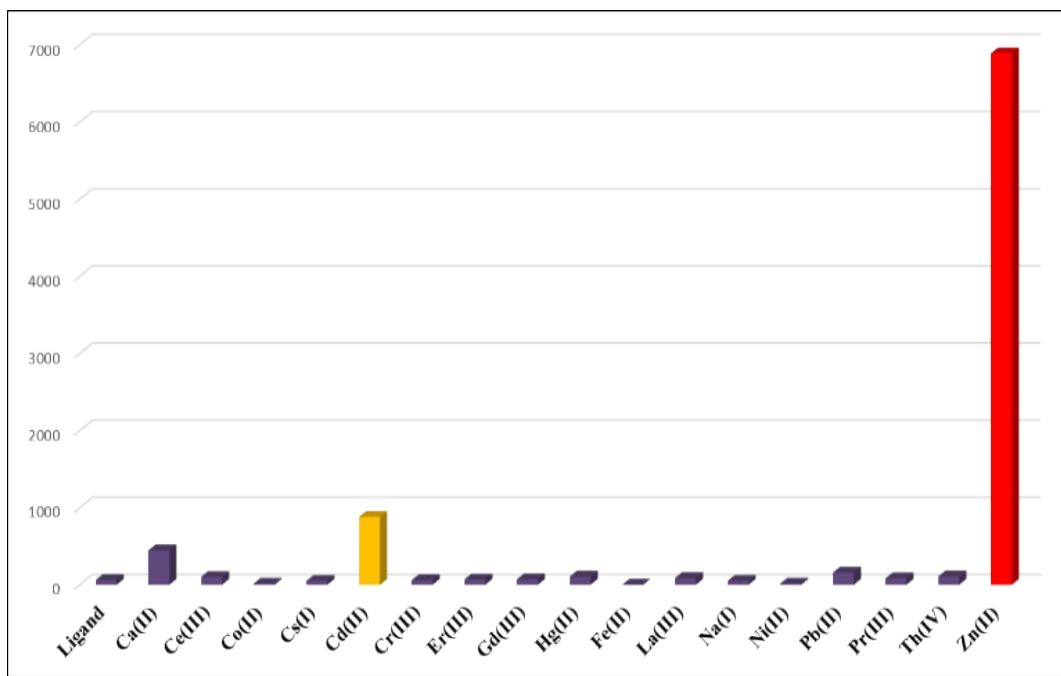


Figure 2S: Bar diagram of fluorescence intensity of alone **L** (1×10^{-5} M) and **L** in the presence of various metal ions of interest (1×10^{-4} M) in $\text{CH}_3\text{CN}-\text{H}_2\text{O}$ (9:1, v/v).

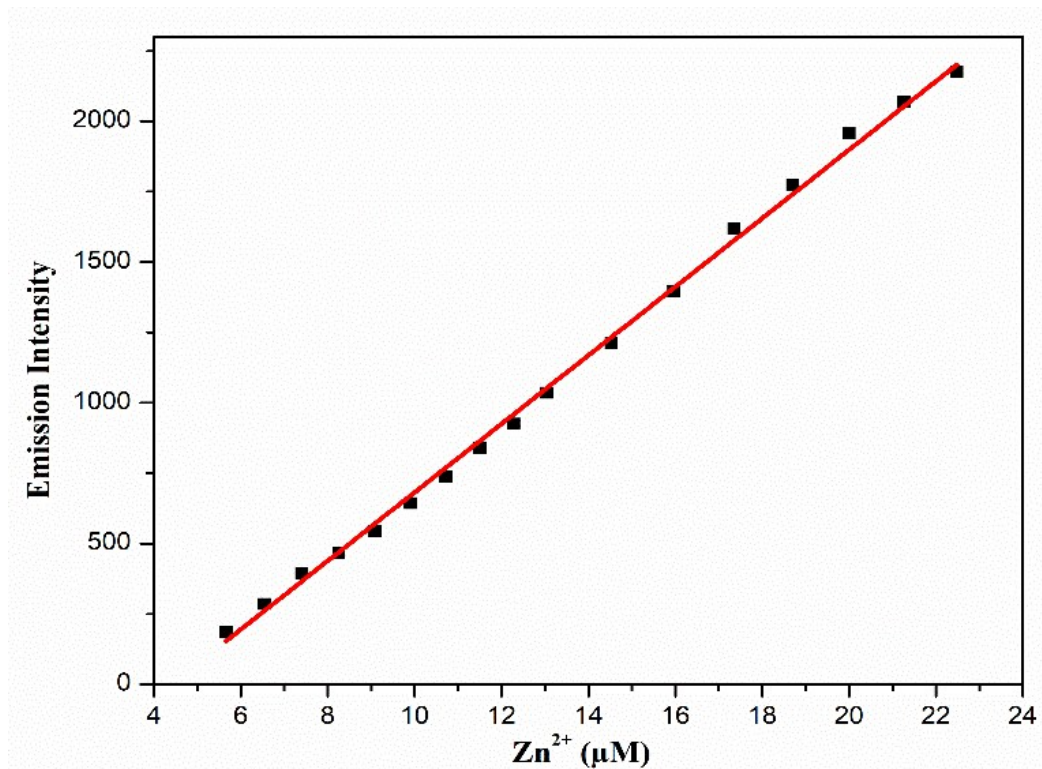


Figure 3S: Calibration plot of **L**- Zn^{2+} in acetonitrile

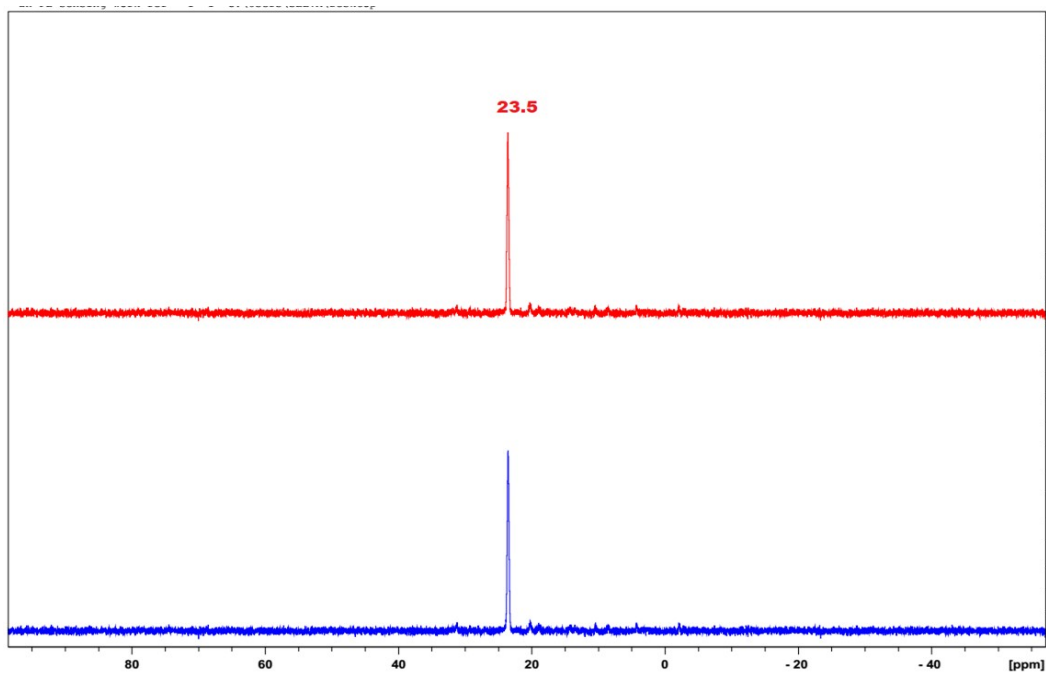


Figure 4S: ^{31}P NMR for **L** and **L-Zn²⁺** in DMSO-d₆.

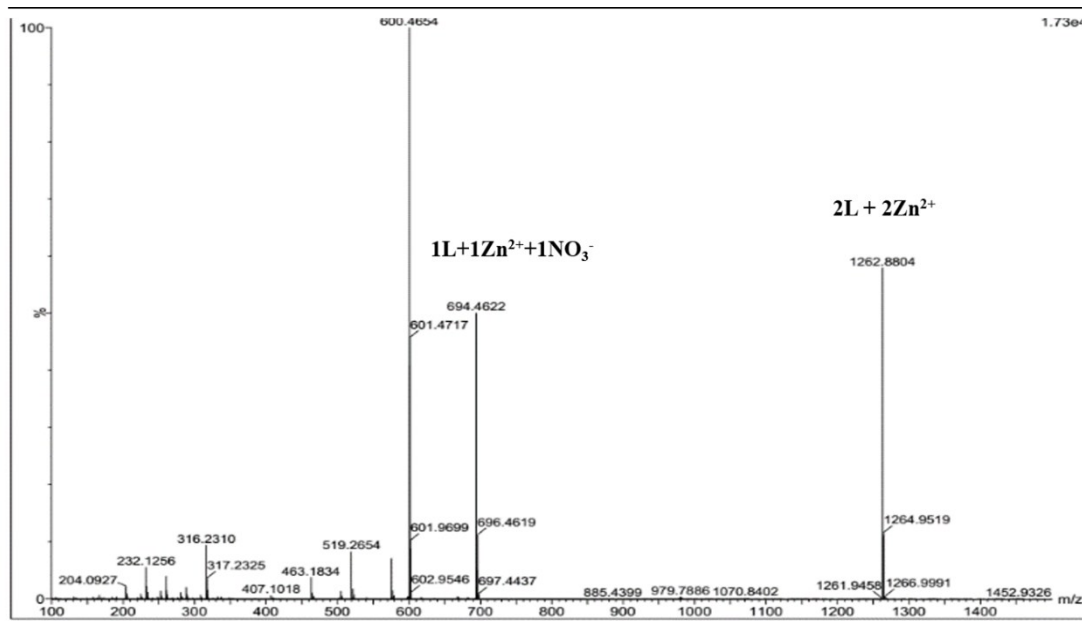


Figure – 5S (b) ESI-TOF mass spectrum for **L-Zn²⁺** complex (ESI-MS exhibited the formation of a complex between **L** and Zn²⁺ [m/z 694.46 (**1L+1Zn²⁺+1NO}_3^{\text{-}}**) m/z 1262.88 (**2L + 2Zn²⁺**)]).

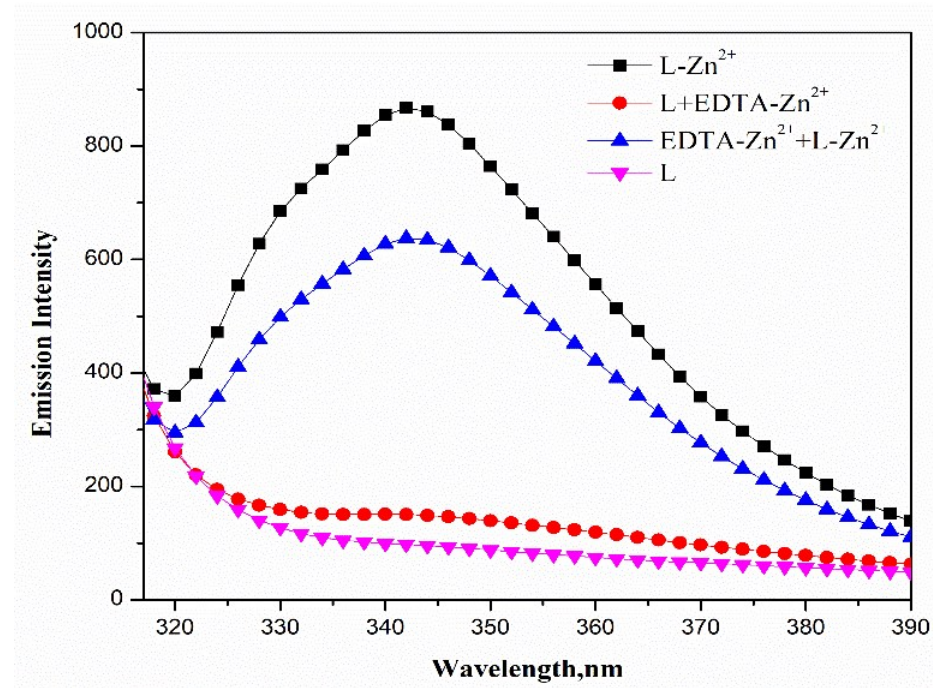


Figure 6S: Reversible changes of optode probe with sequential addition Zn^{2+} and EDTA

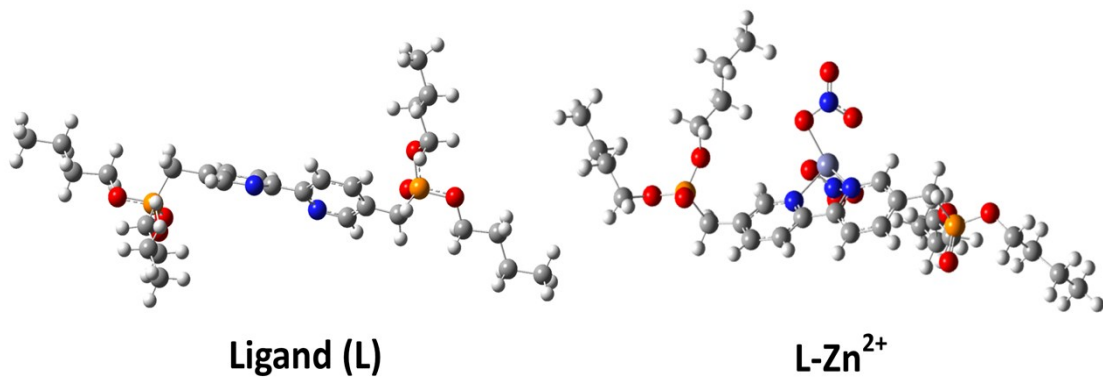


Figure 7S: Optimized structure of **L** and $\mathbf{L-Zn}^{2+}$ complex by DFT/B3LYP method

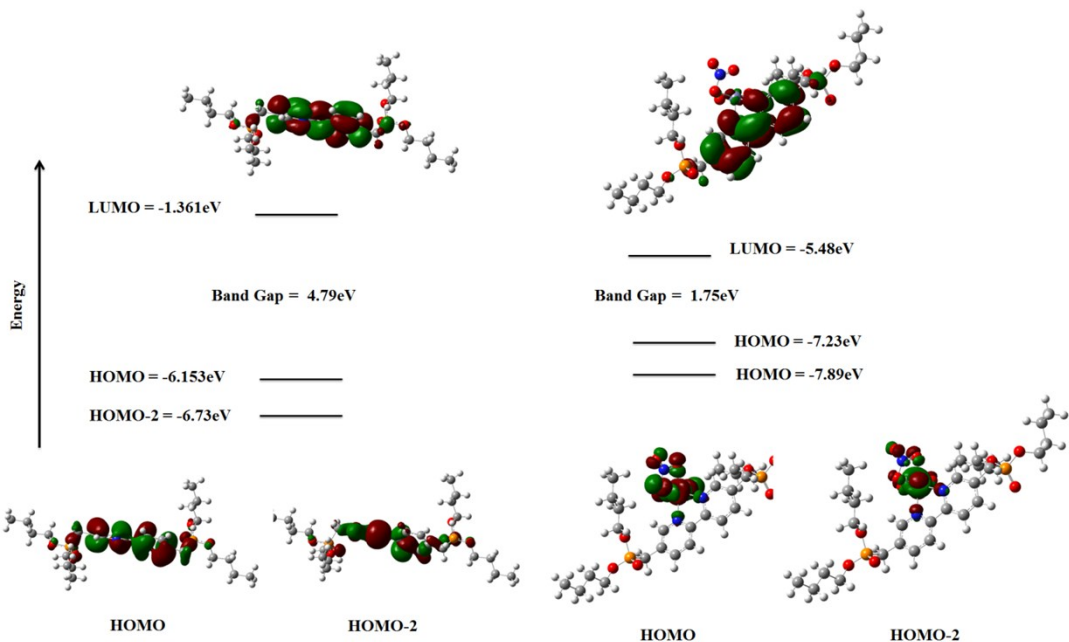


Figure 8S: Calculated HOMO-LUMO of L and L-Zn²⁺ by DFT/B3LYP method.

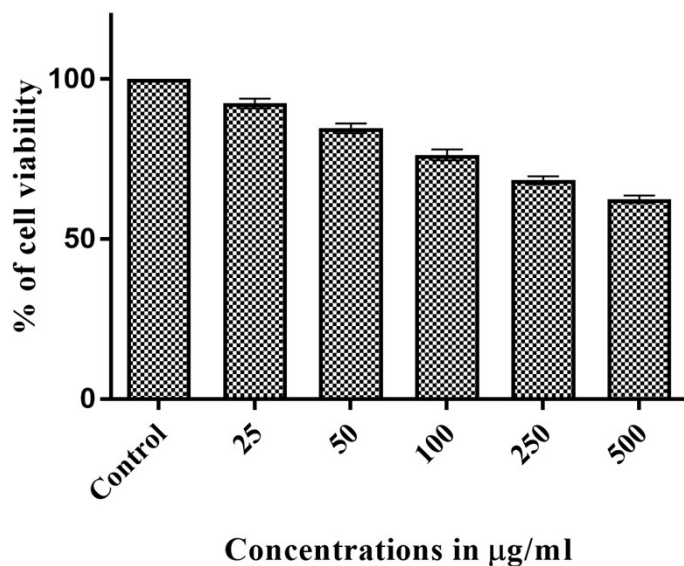


Figure 9S: Cell viability estimated by MTT assay *versus* incubation concentration of cells.

Table 1S: Comparison of optode performance towards Zn^{2+} with previously reported work

S.No	Reagent	Support	Output Signal measured	Limit of Detection (M)	pH	Interference
1	1-octadecyloxy-4-(2-pyridylazo) resorcinol ²⁹	PVC	absorbance	1×10^{-5}	4.8	Cu^{2+}, Co^{2+}
2	1-(2-pyridylazo)-2-naphthol ³⁰	PVC	diffuse reflectance	1.53×10^{-6}	3.9	$Cd^{2+}, Cu^{2+}, Mn^{2+}, Ni^{2+}$
3	1-(2-pyridylazo)-2-naphthol ³¹	Sol-gel	absorbance	2×10^{-6}	5.5	$Pb^{2+}, Fe^{2+}, Cu^{2+}, Cd^{2+}$
4	1-(6-(tert-butyl)-1',3',3'-trimethylspiro[chromene-2,2'-indolin]-8-yl)-N,N'-dimethylmethanamine ³²	PVC	fluorescence	1.51×10^{-7}	7.4	***
5	Zincon ³³	Triacetyl cellulose	absorbance	1.6×10^{-7}	9.0	$Cu^{2+}, Ni^{2+}, Mn^{2+}$
6	4-Benzoxazol-2'-yl-3-hydroxyphenyl allyl ether ³⁴	Silanized glass	fluorescence	4×10^{-5}	7.24	$Cu^{2+}, Co^{2+}, Ni^{2+}$
7	2-(2-hydroxy-5-chloro) benzaldehyde-[4-(3-methyl-3-mesitylcyclobutyl)-1,3-thiazol-2-yl] hydrazone ³⁵	PVC	fluorescence	2.2×10^{-7}	6.0	$Fe^{2+}, Cd^{2+}, Cu^{2+}$
8	1-methyl-1-phenyl-3-[1-hydroxyimino-2-(succinimido) ethyl]cyclobutane ³⁶	PVC	fluorescence	2.5×10^{-8}	6.0	Co^{2+}, Ni^{2+}
9	Dithizone ³⁷	PVC	fluorescence	8.0×10^{-9}	5.0	Hg^{2+}, Ag^{+}
10	1-(p-Nitrophenylazo)-2-naphthol ³⁸	PVC	absorbance	8.0×10^{-7}	9.0	$Cu^{2+}, Co^{2+}, Ni^{2+}$
11	1,5-Diphenylcarbazone ³⁹	Sol-gel	absorbance	1.6×10^{-5}	9.0	$Cu^{2+}, Co^{2+}, Ni^{2+}$
12	tetra butyl 2,2'-bipyridine-5,5'-diybis(methylene)diphosphonate (Present work)	PVC	fluorescence	1.27×10^{-9}	7.0	No interference